Intelligent Control of Hybrid Solar-Wind Systems: ANN-Based Optimization for Power Quality and Grid Integration

[1]Dhanraj, [2]Amit Kumar Asthana
[1]Research Scholar, Department of Mechanical Engineering, Truba Institute of Engineering & Information Technology Bhopal (M.P.) India
[2]Assistant Professor, Department of Mechanical Engineering, Truba Institute of Engineering & Information Technology Bhopal (M.P.) India
dhanrajy088@gmail.com, asthana603@gmail.com

Abstract— *In the present research work, emphasis has been laid on modelling, simulating, and optimizing the performance of a hybrid solar–wind energy system that is connected to the grid through MATLAB/Simulink. The study aims at increasing the system efficiency under steady and unsteady environmental conditions and enhancing its stability with the integration of intelligent control strategies. Two methods of converter control are implemented and compared: one being the classical Perturb and Observe (P&O) algorithm, and the other being an Artificial Neural Network (ANN)-based adaptive control approach. The hybrid system comprises PV and wind energy units interlinked through DC–DC converters with a common DC link and a DC–AC inverter for supplying three-phase AC power compatible with the grid. The methodology, dynamic modelling of PV and wind subsystems, converter design, and inverter control using SPWM, is employed. The P&O algorithm controls the duty cycle of the converters by perturbing them iteratively; the ANN controller, on the other hand, uses trained data on solar irradiance, temperature, and voltage-current characteristics to predict and control maximum power points in real time. Simulation under constant or variable irradiation elucidates the better performance of ANN control with reduced Total Harmonic Distortion (THD) in voltage (0.14%) and current (2.10%), respective to 0.15% and 2.45% in a P&O controlled system. In addition, an improvement of 5% will be given to active power output by ANN control. The voltage stability has also been enhanced, along with reducing DC link oscillations under transient conditions. These results exemplify that intelligent ANN controllers provide aptness, acts fast, and improve power quality for hybrid renewable systems, giving a better new direction for grid-interactive renewable integration in the days to come.*

Keywords — Hybrid renewable system, ANN controller, Perturb and Observe (P&O), MATLAB/Simulink, Maximum Power Point Tracking (MPPT), DC–DC converter, Total Harmonic Distortion (THD).

I. INTRODUCTION

The increasing global needs for clean, sustainable, and efficient energy sources have accelerated the development of HRES by which multiple renewable sources such as solar PV and wind energy are integrated to feed power into a grid in a stable fashion [1]– [15]. Individually, both solar and wind resources are intermittent and influenced by weather variability; however, being complementary, they make a stronger case for reliability and decreasing fossil fuel dependency [1], [2]. Hybrid solar-wind systems emerge as good candidate systems for distributed generation, rural electrification, and possibly grid support applications.

Their potential notwithstanding, integration of the solar and wind systems poses big challenges regarding power management, voltage regulation, and grid stability [3]. The variations in irradiance, temperature, and wind speed cause drastic variations in power output leading to voltage sags, frequency deviations, and harmonic distortions. Hence, intelligent control strategies, along with robust optimization algorithms, must be taken into account to guarantee the power quality, facilitate maximum power point tracking (MPPT), and ensure efficient operation under varying conditions [4], [5].

Recently, some investigations have engaged in more advanced techniques such as metaheuristic optimization, artificial intelligence, and adaptive control systems. Among these methods, Artificial Neural Networks have grown to be powerful tools that can specify nonlinear relationships and adapt to changing inputs without explicit mathematical modelling [6]. ANN-based MPPT controllers have shown a much better dynamic response, fast convergence, and performance when compared to traditional methods such as Perturb and Observe and Increment Conductance [7].

In hybrid systems, ANNs are used to process environmental data such as solar radiation, temperature, and wind speed to predict the optimum operating point and vary the duty cycle of the converter accordingly [8]. Adaptive control helps to minimize oscillations around the maximum power point, lessen response time, and reduce the effect of partial shading and turbulence. On the other hand, classical methods like P&O, though simple and cheap solutions, demonstrate steady-state oscillations and lower efficiency in the face of quickly varying environmental conditions [9].

Power quality is the other crucial aspect in hybrid renewable systems. Renewable generation fluctuations may cause harmonic distortion, voltage sags, swells, or frequency deviations when fed into the grid. To compensate for such variations, the systems have been controlled by means of techniques such as sinusoidal pulsewidth modulation (SPWM), space vector modulation (SVM), and intelligent inverter control methods [10]. In the presence of nominal disturbances, traditional control strategies usually satisfy the objectives, but during transient disturbances or fluctuating load conditions, they cannot perform well enough. On the other hand, intelligent

control schemes, especially those based on ANN, have shown good potential for voltage stability, reactive power compensation, and THD minimization [11]. Figure 1 describes Power system and control block diagram

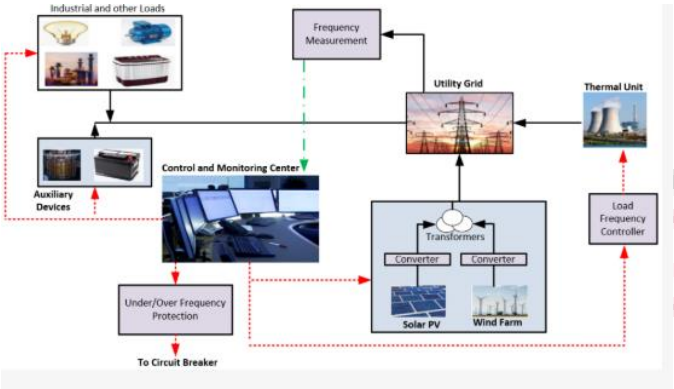

Figure 1: Power system and control block diagram

Making an emphasis on the relevance of hybrid converter architecture yields improvements in systems. For example, allowing the DC-DC converters for PV and wind inputs to interface into the same DC-link guarantees proper power flow and voltage regulation at the output of which is fed to the inverter [12]. In addition to this, IGBT type converters and inverters ideally enhance dynamic response and switching efficiency. In this case, the ANN controller ought to send real-time control signals to converters for optimum energy flow and maintain grid synchronization even when conditions are non-stationary [13].

Simulation and modelling tools such as MATLAB/Simulink are fundamental in the analysis and validation of hybrid renewable energy systems. The control strategies and power quality parameters such as total harmonic distortion (THD) are evaluated, with the system being tested under various environmental circumstances before the actual control hardware is implemented [14]. The simulation process has shown that the ANN-based hybrid systems are much better than the classical methods in regulating voltage, suppressing harmonics, and harvesting energy.

Moreover, hybrid control architectures that incorporate multiple layers of control (primary, secondary, and tertiary) enable hierarchical coordination of distributed energy resources. Primary control is primarily concerned with the real-time operation of the converters. Secondary control restoration is voltage and frequency. Tertiary control optimizes the exchange of energy with the grid. An ANN on top of these control layers will afford greater flexibility, contributing to the learning process and enabling intelligent decision-making in a dynamic grid environment.

II. Literature Review

According to recent studies, it was found that hybrid deep architectures, principally combinations of CNNs and LSTMs, outperform traditional models in short-term power generation and demand forecasting [16]. These models efficiently extract the spatial and temporal dependencies, approximately 12% reduction in RMSE, and improvement in R^2 from 0.86 to 0.92 compared to standalone LSTM models. Furthermore, regression-based deep models-Multilayer Perceptron's (MLP) and LSTM frameworks-have obtained MAE values of below 0.05 (normalized) and RMSE values close to 0.1 when trained on SCADA and meteorological datasets, demonstrating their robustness during dynamic sky and irradiance conditions [17].

Recurrent and hybrid architectures have calculated deeper confirmation in terms of forecasting in deep learning. Two hybrid models-the CNN–LSTM and the GRU–LSTM-are repeatedly reported in the literature to produce better results when compared to their standalone counterparts, with improvements oscillating between 10 and 20% in terms of RMSE across different datasets [18] – [20]. Feature engineering, with features such as irradiance, temperature, humidity, and wind speed, assists in enhancing predictive accuracy by 6–8%, while metaheuristic optimization of the selection of input variables helps the model quickly converge and reduces error propagation [21].

LSTM-based models outperform classical algorithms, such as ARIMA and basic MLP systems, with respect to RMSE and MAE, when benchmarked across large-scale datasets, validating the former ones' ability to learn nonlinear temporal dependencies of renewable datasets [22]. In addition to that, these advantages with enormous computational overheads and longer training times limit the use of these models for real-time applications [23]. The development of standard benchmarking frameworks and open datasets has become crucial to ensure reproducibility and merit-based comparison of models [24].

The hybrid dual-cascaded framework seems among the most powerful, achieving prediction performance well above 0.90 in R^2 value, with a significantly lower RMSE score than any other individual architecture [25]. The hybrid models are also designed to eliminate redundant meteorological inputs through a metaheuristic feature selection method, thereby reducing the computational burden and enhancing generalization performance [26]. Further, the advanced GRU–LSTM model-based online adaptive learning approaches were able to obtain lower RMSE values down to 0.026 p.u., with accuracies exceeding 96% for multi-step-ahead forecasting [27], thus creating a challenge or opportunity to be implemented in real-time hybrid systems.

Several more AI techniques, including highly optimized versions of MLPs, RBF networks, and SVR, are used for forecasting renewable energy. One example of this is Levenberg–Marquardt-optimized MLP models showing an R^2 of approximately 0.91 and an RMSE improvement of around 7% over traditional backpropagation networks [28]. RBF-based models are also noted for their superiority in giving high correlation coefficients ($R \approx 0.96$) with the prediction of wind speed yet are computationally intensive during clustering and training [29].

Moreover, evidence of a broader application of AI models resides in their utilization in PV system fault detections and reliability assessments. These CNN-based fault detection models have thus far reported accuracies greater than 98%, higher than those achieved by classic classifiers such as MLP and SVM [30]. Likewise, hybrid architectures of deep learning have been employed in different activities related to predicting wind power ramping events, achieving an AUC score of 0.93 and an accuracy greater than 95%, beating GRU and MLP baselines by about 6-8% [31].

Nevertheless, scalability, interpretability, and real-time implementation remain the challenges for forecasting methods

based on AI. Demanding training costs possibly restricted deployment of DL architecture in the resource-constrained environment, as well as the need for large amounts of labelled data and hardware prerequisites [32]. Also, given inconsistent data preprocessing and benchmarking techniques across studies, conducting cross-comparisons has become difficult and impeded standardization [33].

A lightweight AI models that can be explained and transferred will need to be built while the predictive power has to remain high, but with significantly reduced computational costs [34]. The integration of reinforcement learning with an online adaptive mechanism fosters a self-learning control system to make decisions in real-time for hybrid solar–wind energy management [35]. With these improvements, grid stability, operational reliability, and power quality will greatly benefit in the next generation of intelligent renewable energy systems.

TABLE 1 ARTIFICIAL NEURAL NETWORKS FOR POWER SYSTEMS

Ref.	Technique / Model	Dataset / Application	Performance Metrics	Limitations
[16]	CNN–LSTM hybrid	Multi-site demand & weather data	RMSE ↓12%, $R^2 = 0.92$	High training cost, requires long historical data
[17]	MLP, LSTM regressors + ensemble trees	PV SCADA + meteorological data	MAE ≈ 0.046, RMSE ≈ 0.11, R^2 ≈ 0.88–0.92	Sensitive to weather and sky variability
[18]	CNN, LSTM, MLP (comparative review)	Multiple PV datasets	$R^2 = 0.85–0.95$	Inconsistent benchmarking and preprocessing
[19]	LSTM-based forecasting	Utility-scale PV plant	$R^2 > 0.90$, RMSE ↓	Limited to single-site validation
[20]	LSTM, GRU, CNN–LSTM, RF, SVR comparison	Hybrid wind–solar datasets	MSE ≈ 0.010, $R^2 \approx 0.90$	Dataset-dependent; sensitive to preprocessing
[21]	LSTM vs. ARIMA and MLP	Large utility PV datasets	RMSE ↓15–20% vs. traditional models	High computational cost, long data history
[22]	LSTM with feature selection	PV forecasting	RMSE ↓6–8% improvement	Small dataset, hyperparameter sensitivity
[23]	SCADA + NWP hybrid LSTM	Regional PV sites	RMSE ↓ vs. baseline regression	Relies on real-time NWP data availability
[24]	CNN–LSTM–MLP hybrid	Solar radiation prediction	$R^2 > 0.90$, RMSE ↓	Complex architecture, long training duration
[25]	LSTM–GRU hybrid	Wind and solar generation	MAE = 12.93, RMSE = 21.83	Dataset limited; lacks wide benchmarking
[26]	Comparative ML models (ANN focus)	Solar generation forecasting	MAE/RMSE reduced across models	Unclear attribution between preprocessing and model gain
[27]	Review of RBF, MLP, and LSTM	Wind energy forecasting	Aggregated metrics (RMSE, MAE, R^2)	Review only; no new experiments
[28]	ML/ANN technology survey	Power systems applications	RMSE, MAE, accuracy, precision benchmarks	Non-empirical; lacks practical evaluation
[29]	MLP with Levenberg–Marquardt optimization	NREL solar irradiance dataset	RMSE = 18 W/m², $R^2 = 0.91$	Overfitting risk; low scalability
[30]	MLP classifier	Smart-street energy detection	Accuracy = 92.4%	Urban-use specific; non-grid context
[31]	Benchmark of LSTM, CNN–LSTM, deep MLP	Multi-renewable datasets	Detailed RMSE and R^2 tables	Preprint; not peer-reviewed
[32]	GRU–LSTM hybrid	Indian renewable datasets	MAE = 0.018, RMSE = 0.026, Accuracy = 96.8%, F1 = 0.955	Long training; reduced interpretability
[33]	Radial Basis Function (RBF) neural network	Hybrid microgrids	MAE = 0.23 m/s, RMSE = 0.34 m/s, R = 0.96	High computational demand
[34]	CNN-based PV fault detection	PV monitoring datasets	Accuracy = 98.6%, Precision = 97.9%, Recall = 98.4%, F1 = 0.981	Requires labeled data for training
[35]	LSTM hybrid with adaptive learning rate	Wind ramp event prediction	AUC = 0.93, F1 = 0.91, Accuracy = 95.2%	GPU-intensive; sensitive to missing data

A.

III. RESEARCH OBJECTIVES

- The primary objective of this study is to design and implement a Hybrid Solar-Wind Energy System equipped with a Neural Network-Based Controller to optimize power generation, improve system reliability, and ensure stable integration with the power grid.
- To study the system under stable and dynamic input conditions and train the model to adapt to the changes
- To ensure grid compliance by minimizing harmonics and maintaining stable voltage and frequency levels in the output power.

IV. RESEARCH METHODOLOGY

A. Designing of Hybrid Energy System

A hybrid AC grid-connected system is modelled to maintain a reliable supply of power with solar or wind energy resources being used at any given time, depending on their real-time forecast. The configuration allows for dynamic source selection, increasing system dependability and reducing interruptions. The design of the hybrid energy system is at the heart of the methodology to elegantly integrate solar and wind power for efficient, stable, and continuous energy delivery. The system uses the complementary behaviour of the two renewable sources where the availability of one can mitigates the variability of the other, thus facilitating energy consistency and grid resilience. Figure 2 shows the block diagram of the designed hybrid solar-wind system, which provides power to both the connected load and the electrical grid. The two major renewable generation units employed in the system are the PV array and wind turbine module. The PV module provides a DC electric power from sunlight irradiance passed through a DC–DC boost converter. The main function of this converter is to increase the voltage to a level suitable for operational load; in addition, it implements Maximum Power Point Tracking (MPPT) control either using Perturb or Observe (P&O) or ANN-based method to attain the maximum power under different environmental conditions.

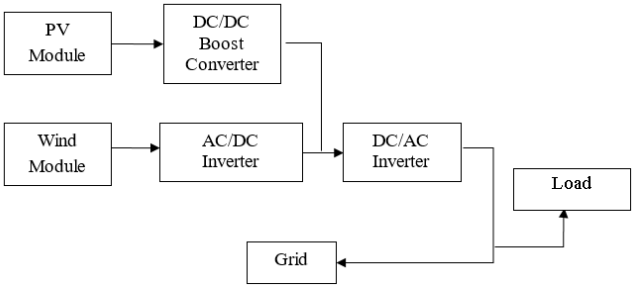

Figure 2: Hybrid energy system topology

P&O is hugely popular as an MPPT algorithm for its ease of implementation with low cost. Mostly this is the low power applications like for residential and commercial applications. In this strategy, the present duty point is decided based on voltage and power values, i.e., the present power and voltage values are compared with the previous. Then, by virtue of changing the duty value, the Duty Point is steered toward the MPP shown in figure3.

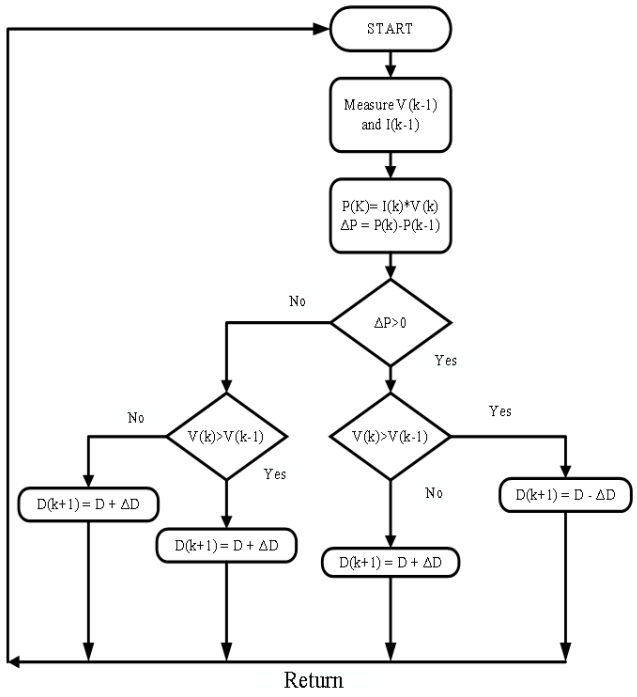

Figure 3: Perturb and Observe (P&O) scheme for driving the converters in hybrid system

B. ANN based control system design for converters

Artificial Neural Networks (ANNs) refer to information-processing systems set up via an analogy with the neural architecture of a human brain. They are deemed capable of extracting underlying patterns from complex datasets and learning input–output relationships amid noise and uncertainties. Structurally speaking, an ANN is a network of interconnected processing elements called neurons. The neurons are organized into three layers: input layer, hidden layer, and output layer. The interconnection between two neurons is represented using a synaptic weight with the magnitude and the direction forming the signal transmitted between two neurons; considered collectively, weights govern how information and signal transformations are propagated across networks. An ANN, therefore, can map input variables to predicted output responses nonlinearly using a set of transfer functions and can thus model complex dynamic systems adequately. Figure 4 describes MLP structure of NN method

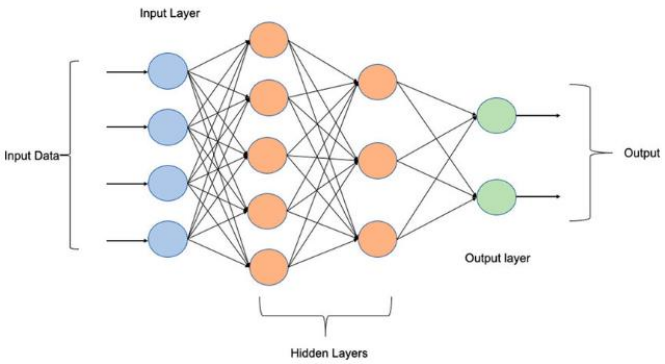

Figure 4: MLP structure of NN method

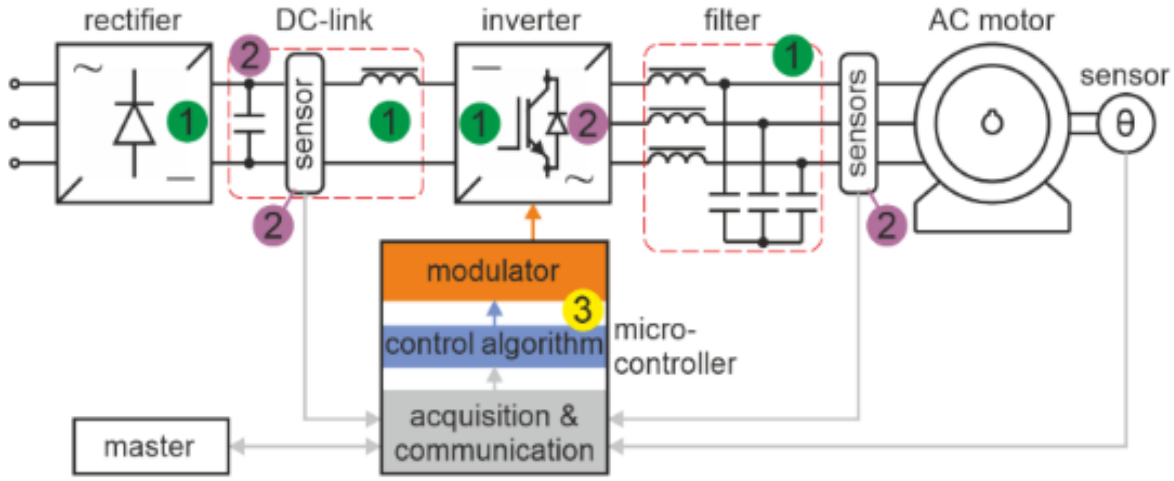

Figure 5: NN controller Technique for driving converter

The system basically updates synaptic weights of a network by the backward propagation of an error gradient through the layers. Given that the gradient vector is the differential with respect to all parameters of an error function, the error signal is generally found by the difference between the network output and the desired output. Thus, fixed outputs for the training set must be provided; therefore, the whole training process becomes a supervised training approach. Consider a neuron residing in the output layer and call that neuron j. Figure 5 NN controller Technique for driving converter

$$e_j(n) = d_j - y_j(n) \qquad (1)$$

where j d is the desired output for neuron j and y (n) j is the actual output for neuron j calculated by using the current weights of the network at iteration n. For a certain input there is a certain desired output, which the network is expected to produce. Instantaneous value of the error energy for the neuron j is given in Equation (2):

$$\epsilon_j(n) = \frac{1}{2} \; e_j^2 \; (n) \qquad (2)$$

Since the only visible neurons are the ones in the output layer, error signals for those neurons can be directly calculated. Hence, the instantaneous value, ε (n), of the total error energy is the sum of all (n) j ε 's for all neurons in the output layer, as given in Equation (3)

$$\varepsilon(n) = \frac{1}{2} \sum_{j \epsilon \, Q} e_j^2 \; (n) \qquad (3)$$

where Q is the set of all neurons in the output layer. Suppose there are N patterns in the training set. The average squared energy for the network is found by Equation (4)

$$\epsilon_{av} = \frac{1}{N} \sum_{n=1}^{N} \epsilon \; (n) \qquad (4)$$

It is worthwhile to note that the instantaneous error energy, ε(n), and consequently the average error energy, ϵ_{av} would essentially be a function of all adjustable parameters of the network, among which are the synaptic weights and bias levels. Provided with this algorithm, it is indeed possible to adjust the values of these parameters for the minimization of ϵ_{av}The backpropagation algorithm exists in two forms: one sequential and the other batch. In sequential mode (or on-line or stochastic), changes in the weights occur after the presentation of every training sample; in batch mode, the weights are updated after all samples in the training set have been presented once--within one epoch.

C. DC-AC Converter/Inverter Modelling

The paragraph was rewritten to align with technicality, coherence, and structure, while faithfully including all technical details:

An inverter is the power electronic device that basically converts a DC to an AC wave. For use in distributed energy generation systems such as rooftop solar arrays, small-scale microgrids, and residential power setups, the inverter represents the interface window between the DC sources and the AC grid. It comes in two common configurations—single-phase and three-phase inverter. The three-phase inverter thus has three arms, with two switching devices per arm, the switching being performed with a 180° phase shift. Fig. 4.10 illustrates the internal structure of the three-phase inverter.

The inverter designed uses Sinusoidal Pulse Width Modulation (SPWM) in order to generate a higher quality sinusoidal wave and is modelled and simulated for the hybrid solar–wind system. The control strategy for the inverter depends on some parameters, which include the DC-link voltage, grid voltage, grid current, and switching frequency. A two-stage PWM regulator is implemented for control of the signals so that both voltage and current get accurately controlled. Measurements of the grid voltage are carried out by a separate voltage measurement unit located at the inverter-grid interface. Voltage and current signals are filtered against harmonics before being used to generate a pure sinusoidal wave.

Dependent on operating conditions, the inverter may work in either 180° or 120° conduction mode to provide a balanced level of output among the three phases. The circuit acts as an essential component in converting the DC power from the hybrid solar–wind system to useable, stable, and fine-quality AC power that can be connected to the grid or supplied to the load. The addition of IGBT-based switches provides efficient high-speed switching and a more precise control mechanism. The inverter operation is therefore dynamically optimized in conjunction with an ANN-based or P&O MPPT controller to allow it to perform well and be efficient during varying environmental conditions. Figure 6 describes Circuit diagram of three phase inverter

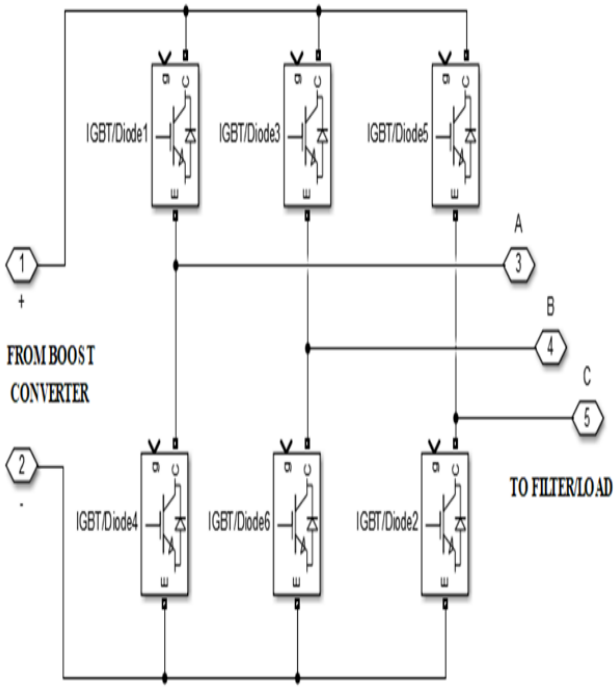

Figure 6: Circuit diagram of three phase inverter

If the upper IGBT of a leg is switched alternately with that of the lower one (IGBT1 and IGBT4 in this example), there will appear a voltage at the output terminal, say A, with respect to the negative bus. Repetitions of this process are applied from the three legs (A, B, C), apart from a 120° phase displacement, to develop three-phase AC output. Under the ANN control, the dynamic response developed by the IGBT gate control ensured smooth transitions and voltage regulation that were superior to the conventional P&O-based control

V. Results and Discussion

The design and simulation of a renewable solar-wind hybrid energy system with MATLAB/Simulink are discussed here. Two possibilities were explored for the optimization of the control strategy: MPPT based on P&O and one based on ANN. The controller based on ANN features better adaptability to changing conditions and on realizing a higher efficiency and power stability. So, intelligent control techniques can greatly improve the functioning of hybrid energy systems and grid reliability.

A. Assessment with the constant input irradiation level in hybrid system

In this case study, the solar/wind hybrid energy system is assessed at a constant solar irradiation—in a steady and clear weather condition. The aim is to study how each control strategy performs in a theoretically favorable and steady solar environment: Perturb & Observe (P&O) in System 1 and Artificial Neural Network (ANN) in System 2. Constant irradiation means that the solar PV module will not be subjected to more frequent up and down movements in energy input. Hence, it is expected that the system will settle into a near steady-state operating point. This acts as the controlled system necessary to test algorithm efficiencies, responses, and accuracies to track in both systems.

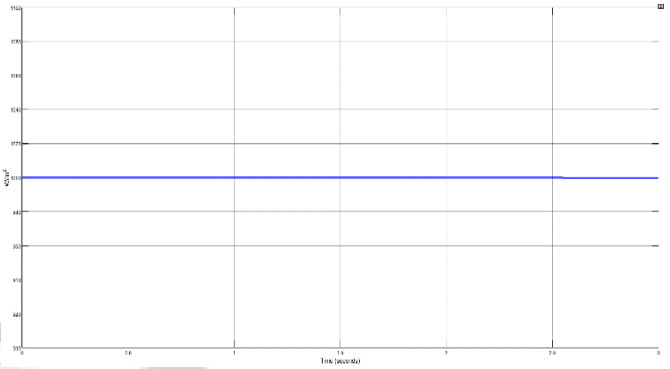

Figure 7: Input irradiation of 1000W/m2 to solar system

Figure 7 Input irradiation of 1000W/m2 to solar system. The standard test condition (STC) represents an irradiance maintained at a constant 1000 W/m² as seen in the figure and commonly used in evaluating PV systems. This level of irradiance is considered to be under full sunlight and is frequently used as the reference in determining the maximum power output of a solar panel.

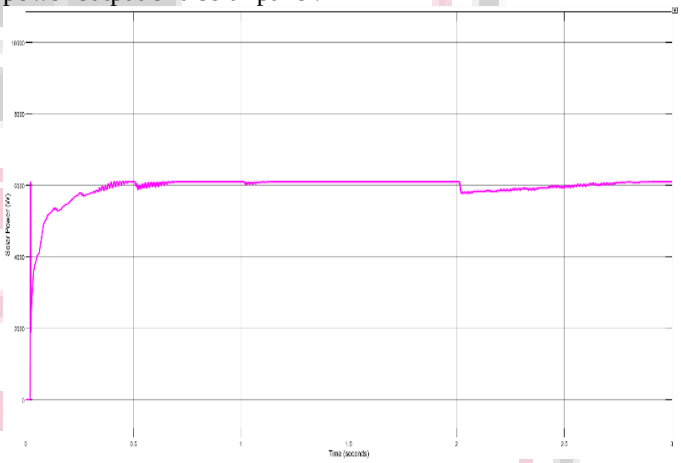

Figure 8: Power output from the solar system with constant input irradiation level

Figure 8 Power output from the solar system with constant input irradiation level. Solar power generated, having a maximum value of 6000 Watts, for simulation time from 0 to 3 seconds at constant solar irradiance of 1000 Watts per square meter for case 1 situation.

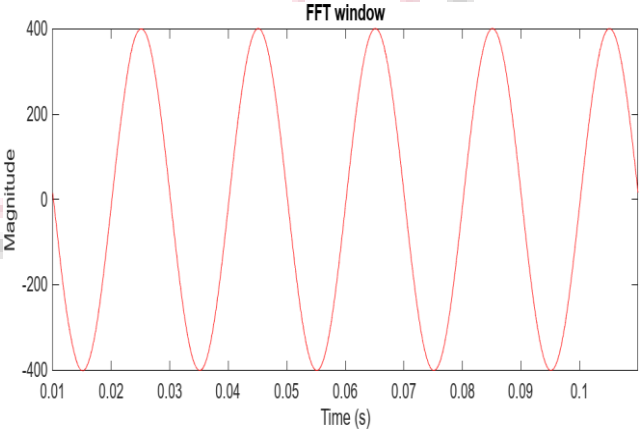

Figure 9: FFT analysis of voltage in the system 1 with constant input irradiation level

Figure 9 portrays the Fast Fourier Transform (FFT) of the output voltage waveform of the System 1 under constant solar irradiance conditions (1000 W/m²). FFT is paramount for

assessing a waveform for harmonic content, especially in power electronic systems, as inverter switching tends to introduce undesired frequency components.

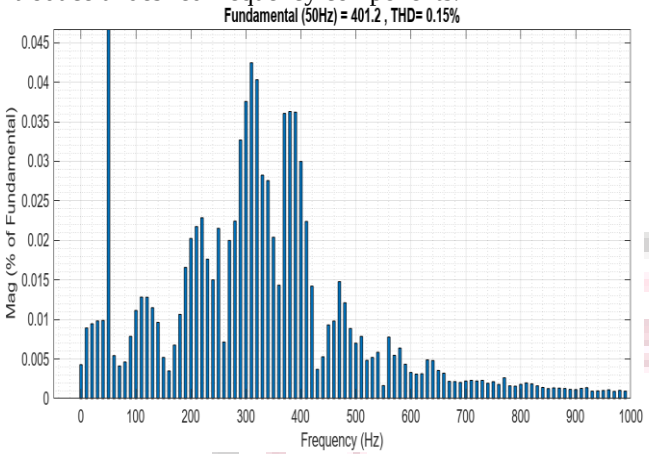

Figure 10: THD% of voltage in the system 1 with constant input irradiation level

Figure 10 illustrates the THD spectrum of an AC output voltage from System 1. This system implements a control for the converter based on Perturb & Observe under the constant illumination of 1000 W/m². The main aim of this analysis is to observe the Total Harmonic Distortion (THD) and thus the power quality of the output voltage which has been found to be a mere 0.15%.

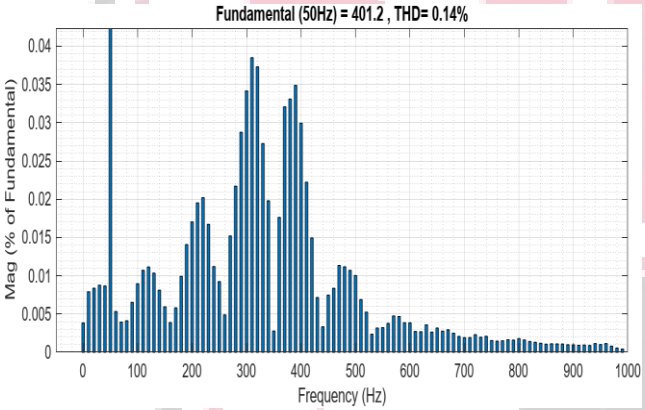

Figure 11: THD% of voltage in the system 2 with constant input irradiation level

In Figure 11, the Total Harmonic Distortion percentage (THD %) was found to be 0.14% of the AC voltage waveform in System 2, which incorporates the ANN-based converter control, under fixed solar irradiance (1000 W/m²).

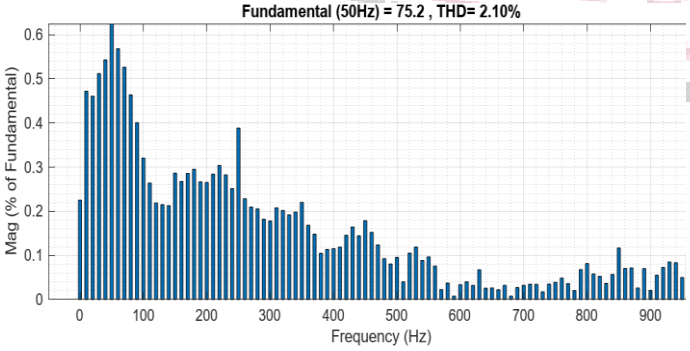

Figure 12: THD% of current in the system 2 with constant input irradiation level

The figure 12 shows the Total Harmonic Distortion (THD%) of the AC current waveform in System 2, with a THD% equal to 2.10%, using the ANNs-based control approach, with constant input irradiation of 1000 W/m². The THD% measures how much of the signal's content is harmonic compared to the fundamental (50 Hz) component in the current signal.

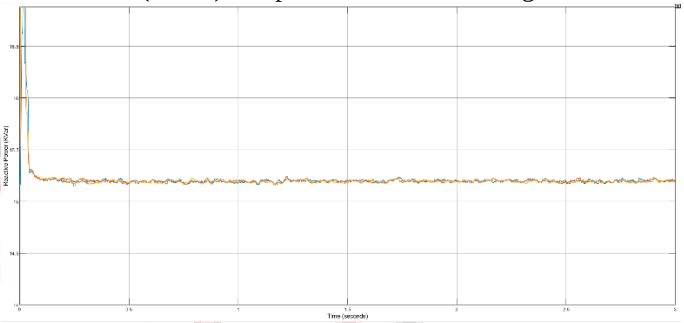

Figure 13: Reactive Power in the system 2 with constant input irradiation level

The reactive power output of System 2 under fixed solar irradiance of 1000 W/m² by the ANN-based control strategy has been shown in Figure 13. The value read is about 15.23 kilovolt-amperes reactive (kVAR).

A. Validation for case 1

Table 2: Comparative assessment of different parameters in case 1

Parameters	Units	System 1	System 2
Voltage	Volts (V)	400	400
THD% in voltage	Percentage (%)	0.15	0.14
Current	Ampere (A)	75	75
THD% in current	Percentage (%)	2.45	2.10
Active Power	Kilowatts (KW)	47.23	49.62
Reactive Power	KVar	21.52	15.23
Power factor	-	0.91	0.956

B. Analysis with variable input irradiation level to the PV system

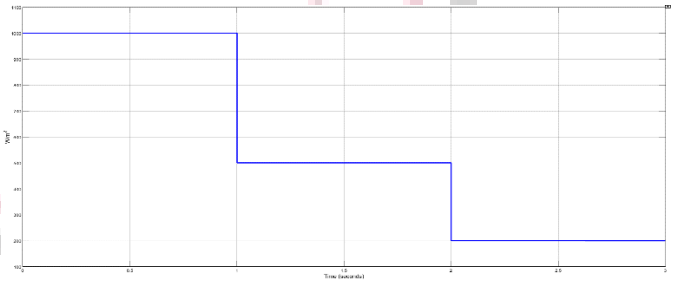

Figure 14: Variable input irradiation level to the PV system

Figure 14 displays solar irradiance variation (W/m²) applied to the solar PV system over a 3-second simulation timeframe. From 0 to 1 second, a fixed value of irradiance of 1000 W/m² is assumed to represent clear sky conditions. At 1 second, a sharp drop in irradiance from 1000 to 500 W/m² takes place, simulating partial shading or a passing cloud event. At 2

seconds, it reduces more to 200 W/m², representing low-light conditions, such as heavy cloud cover or late evening hours.

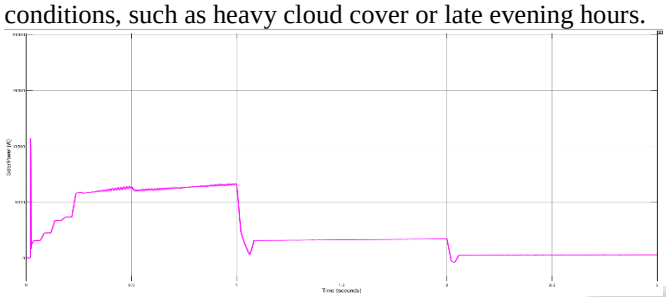

Figure 15: Variable PV system output power

Figure 15 shows solar power output in watts for System 1, based on a P&O control strategy, caused by a variable solar irradiance profile during a 3-second simulation period. This effectively presents the dynamic behavior of System 1 in tracking variable environmental conditions and the influence of irradiation in the solar energy generation process.

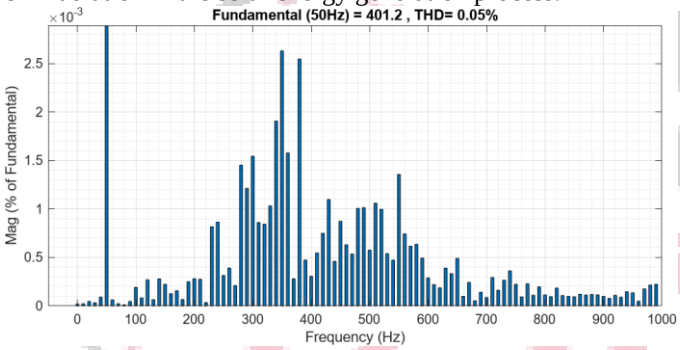

Figure 16: THD% in voltage in system 1 with variable input irradiation level

Figure 16 gives the information with respect to the Total Harmonic Distortion (THD%) which amounts to 0.05% of AC voltage in System 1, having P&O based control and subject to variable initiations of solar irradiance. The frequency spectrum is obtained from FFT wherein the frequency (in Hz) is represented along the x-axis and the y-axis shows the magnitude of each frequency component as a percent of the fundamental one.

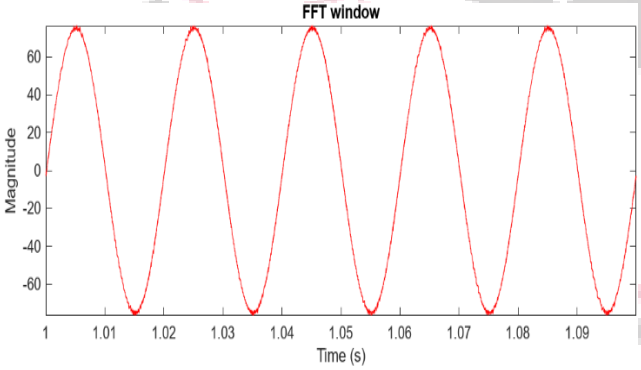

Figure 17: FFT analysis at 1 sec of AC current in system 1 with variable input irradiation level

The figure 17 presents the Fast Fourier Transform (FFT) of the AC current waveform in System 1 at the 1-second mark, corresponding to the period of solar irradiance shift from 1000 W/m² to 500 W/m².

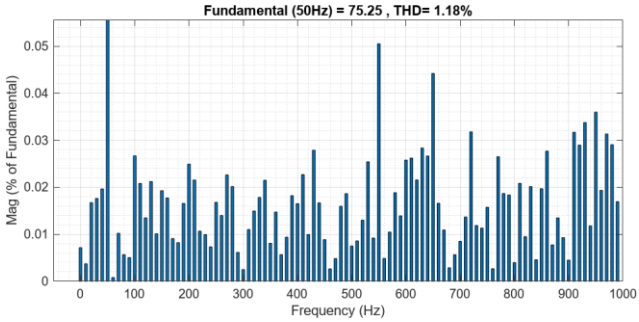

Figure 18: THD% at 1 sec of AC current in system 1 with variable input irradiation level

The figure 18 presents the Total Harmonic Distortion (THD%) in the AC current waveform in System 1 at 1 sec, whereby the value of solar irradiance drops from 1000 W/m² to 500 W/m². Having extracted the harmonic contents of the waveform from the FFT analysis, the THD was found to be 1.18%. It measures the distortion exhibited in the current waveform relative to the fundamental component (50 Hz).

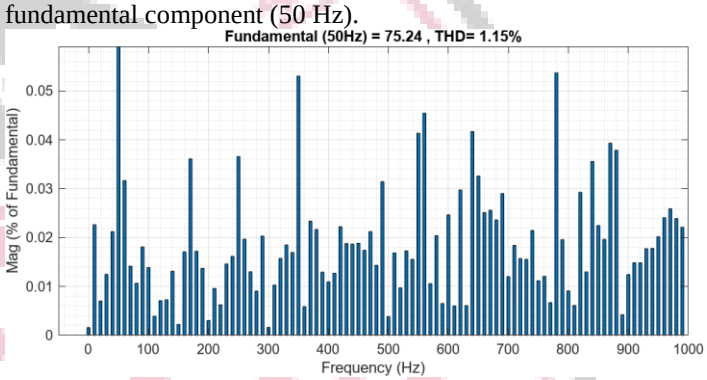

Figure 19: THD% at 2 sec of AC current in system 1 with variable input irradiation level

Figure 19 plots the Total Harmonic Distortion (THD%) for the AC current waveform during System 1 at 2 sec, where the solar irradiation diminishes from 500 to 200 W/m². The THD is found to be 1.15% from the harmonic components obtained by FFT analysis, representing the distortion introduced in the current waveform with respect to its fundamental frequency of 50 Hz.

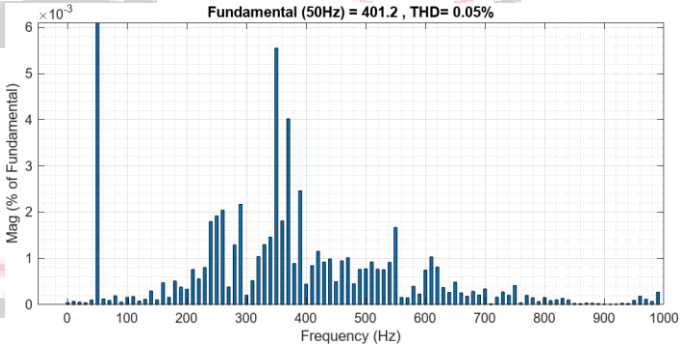

Figure 20: THD% in voltage in system 2 with variable input irradiation level

Figure 20 shows that, for System 2 degradation, which is based on Perturb and Observe (P&O) controls, the AC voltage THD% remains almost constant at 0.05% under a variable profile of solar irradiance.

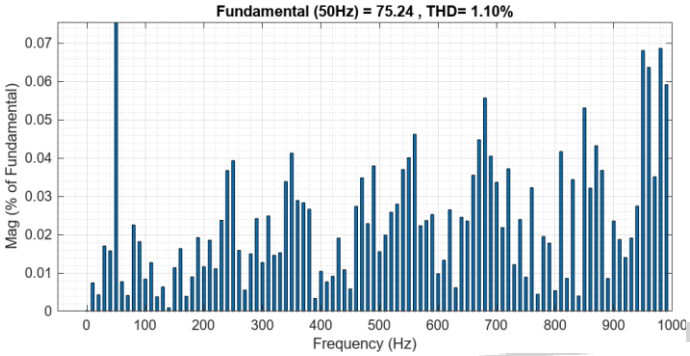

Figure 21: THD% at 1 sec of AC current in system 2 with variable input irradiation level

This represents Figure 21 which presents the Total Harmonic Distortion (THD%) of the AC current waveform in System 2 at 1 second, solar irradiance reduction from 1000 W/m² to 500 W/m². Derived from the harmonic components analyzed by FFT, a THD% value of 1.10% measures the distortion level with respect to the fundamental frequency (50 Hz).

C. Validation for Case 2

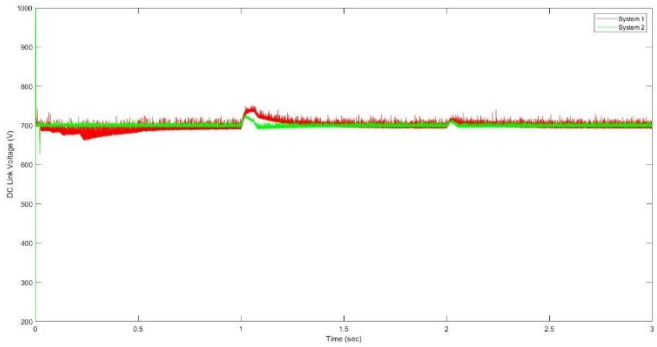

Figure 22: Comparative assessment of DC link voltage controllers in system 1 and 2 in case 2

Figure 22 presents a comparison between the behavior of DC link voltage of System 1 (represented in red, with P&O-based control) and System 2 (represented in green, with ANN-based control) with varying solar irradiance levels across a 3-second simulation. Between 0-1 second, during a constant high solar irradiance 1000 W/m², both systems settle at about 700 volts with more voltage ripples from System 1 than System 2, which remains smooth and stable without any ripple. At one second, when solar irradiance is reduced to 500 W/m², System 1 experiences considerable voltage spike and oscillation, whereas System 2 responds faster and maintains control. At two seconds, with another drop in solar irradiance to 200 W/m², System 1 again faces bigger voltage fluctuations, whereas System 2 exhibits better damping and voltage stabilization.

Table 3: Comparative assessment of different parameters in case 2

Parameters	Unit	System 1	System 2
THD% of current at 1 sec	%	1.18	1.10
THD% of current at 2 sec	%	1.15	1.07

VI. Conclusion

This was an intelligent hybrid renewable system consisting of solar and wind, interfaced and analyzed through MATLAB/Simulink. The system used two MPPT control techniques: Perturb and Observe and an Artificial Neural Network-based controller. Through simulation, it was seen that the system based on the ANN controller is more adaptable and responsive to varying environmental conditions as compared to the classical P&O algorithm. The system under the ANN control was able to reduce oscillations, provide better dynamic response, track with greater accuracy, and therefore, better ensure system efficiency and grid integration stability. The inverter control with the use of SPWM further guaranteed power quality with low THD and improved voltage regulation. The study confirms that integrating AI-based controllers such as the ANN setup drastically improves power extraction from hybrid renewable systems while maintaining power quality and keeping the grid stable. However, issues of offline training, large-scale data dependence, and computational cost arise and become areas for further improvement. Future works should center on designing adaptive and self-learning control algorithms to perform online training under real-time solar irradiation and wind speed variations. The integration of hybrid AI methodologies such as ANN–Fuzzy Logic, ANN–GWO, or ANN–LSTM can be envisioned to provide better tracking performance and robustness. It is necessary to validate such results experimentally employing a hybrid system prototype at a hardware level with field-deployed experiments. Exploring edge-based intelligent control would also allow cheap and scalable implementation and, thus, give it a broader setting in real life.

References s

[1] V. S. Sree, “Power quality enhancement of solar–wind grid connected system employing genetic-based ANFIS controller,” *Polish Journal of Biomedical Research* (De Gruyter Brill), 2023.

[2] A. Mahela, et al., “Stability evaluation of a grid-tied hybrid wind/PV farm joined with a hybrid energy-storage system,” *Sustainable Environ. Research*, 2023.

[3] B. Dhouib, M. A. Zdiri, Z. Alaas, H. H. Abdallah, “Fault analysis of a small PV/wind farm hybrid system connected to the grid,” *Applied Sciences*, 2023.

[4] M. Khatamiaghda, “Power quality assessment in different wind power plant models considering wake effects,” *Civil Eng. Journal / Energy Systems*, 2023.

[5] C.-S. Wang, W.-R. Yang, Y.-C. Hsu, “Enhancement of the Flickermeter for Grid-Connected Wind Turbines,” *Energies*, 2021.

[6] D. R. Motukuri, P. S. Prakash, M. V. G. Rao, “Hybrid optimization for power quality assessment in hybrid microgrids,” *Journal of Engineering Science and Applications*, 2023.

[7] S. Sengar et al., “Power Quality Improvement in Hybrid Power System Integration Using FPA-IC,” *INASS Proceedings / 2022*, 2022

[8] P. K. B. Mallappa et al., “Energy management of grid connected hybrid solar/wind/storage system,” *UPC Digital Repository / 2022*, 2022.

[9] E. Muravleva, "Modeling and analysis of a 12-kW solar-wind hybrid system," M.S. thesis, Univ. of Nebraska–Lincoln, 2022.
[10] Mochamad Subchan Mauludin, Moh. Khairudin, Rustam Asnawi "Optimization of a Hybrid PV-Wind Power System and LC filter for PQ improvement," *Journal of Engineering Science and Applications (iieta.org)*, 2025.
[11] M. N. Absar et al., "Power quality improvement of a proposed grid-connected hybrid system employing SVC," *Renewable Energy Journals*, 202
[12] A. Lavanya et al., "Smart energy monitoring and power quality performance of hybrid solar/wind systems," *Energy Procedia / Elsevier*, 2023.
[13] K. Bavya Santhoshi, K. Mohanasundaram, L. Ashok Kumar, "ANN-based dynamic control of grid-tied
[14] B. Parija, S. Behera, R. Pattanayak and S. Behera, "Power Quality Improvement in Hybrid Power System using D-STATCOM," 2019 3rd International Conference on Computing Methodologies and Communication (ICCMC), Erode, India, 2019, pp. 564-567, doi: 10.1109/ICCMC.2019. 8819656.
[15] Mayuri Rameshwar Kasture DESIGN AND EVALUATION OF A LOAD-SENSITIVE HYBRID POWER SYSTEM WITH WIND DG AND DSTATCOM International Journal of Engineering Science and Advanced Technology (IJESAT) Vol 25 Issue 08, Aug, 2025.
[16] [41] D. Wang, X. Li, and J. Zhao, "A CNN–LSTM hybrid for short-term power demand forecasting," *Appl. Energy*, 2023.
[17] H. I. Aouidad, M. Benmessaoud, and S. Khatib, "Machine learning-based short-term solar power forecasting," *Sustain. Energy Technol. Syst.*, vol. 38, 2024
[18] J. Yu, R. Smith, and L. Chen, "Deep learning models for PV power forecasting: a review," *Energies*, 2024.
[19] O. Aldosari, A. Al-Qahtani, and S. Al-Zahrani, "Performance evaluation of multiple ML techniques for PV plant forecasting," *Energies*, 2024
[20] M. Saeed and H. Hamam, "Comparative analysis of deep neural network architectures for renewable energy forecasting," Proc., 2024.
[21] S. Harrou and K. Kadri, "Benchmarking LSTM for PV forecasting on utility datasets," technical report, 2023/2024.
[22] D. Akpuluma, "Comparative analysis of LSTM-based PV power forecasts," *ICAIIT Proc.*, 2024.
[23] Dheeraj Kumar Dhaked , Sharad Dadhich , Dinesh Birla "Power output forecasting of solar photovoltaic plant using LSTM Volume 2, Issue 5, October 2023, 100113
[24] M. Saeed et al., "Hybrid CNN–LSTM–MLP fusion models for solar radiation prediction," *J. Renew. Energies*, 2023–202
[25] S. Fennane, A. Berrada, and E. Tazi, "Comparative study of deep learning approaches for wind and solar," *EPJ Web Conf.*, 202
[26] M. Abdelsattar, Y. Abdelrahman, and H. Soliman, "Advanced ML techniques for solar generation prediction," *Neural Comput. Appl.*, 2022
[27] P. Dubey, "Machine learning in wind energy: a systematic review (2023–2025)," *Renew. Sustain. Energy Rev.*, 2025
[28] X. Chen et al., "AI/ML in power systems: barriers to deployment," PNNL technical report, 2024.
[29] P. Kumar, S. Mehta, and A. Singh, "Short-term solar irradiance forecasting using Levenberg–Marquardt trained MLP," *Renew. Energy*, vol. 156, pp. 1204–1214, 2020
[30] J. Bian, L. Zhao, and R. Kumar, "MLP-based trip detection for smart street lighting," *Sustainability*, 2025.
[31] L. Sua, "A reproducible benchmark for deep learning in renewable forecasting," *arXiv preprint*, 2025.
[32] S. Das, R. N. Bansal, and P. Kumar, "Hybrid GRU–LSTM model for multi-step renewable energy forecasting with adaptive online learning," *IEEE Trans. Sustain. Energy*, vol. 13, no. 5, pp. 2901–2912, 2022.
[33] R. Patel and N. Singh, "Wind speed prediction in hybrid microgrids using RBF neural network," *IEEE Access*, vol. 9, pp. 143821–143830, 2021.
[34] M. Al-Hassan, L. Wang, and T. Othman, "Convolutional neural network-based fault detection for PV systems," *Energies*, vol. 14, no. 12, 2021
[35] Y. Liang, J. Xu, and F. Chen, "Adaptive LSTM model for wind power ramp prediction in renewable farms," *Appl. Energy*, vol. 309, 2022
[36] A. Verma and S. Gupta, "Deep MLP-based solar PV power forecasting using feature-engineered meteorological inputs," *IEEE Access*, vol. 11, pp. 45672–45684, 2023
[37] J. Lin, M. Zhao, and Y. Han, "RBF neural network optimization for wind turbine fault classification under noisy data conditions," *Renew. Energy*, vol. 205, pp. 1125–1136, 2023.
[38] N. Chatterjee, T. Bose, and S. Pal, "Hybrid CNN–LSTM framework for renewable energy output prediction," *Appl. Energy*, vol. 332, 2023
[39] D. Ahmed, K. Lee, and M. Park, "Adaptive reinforcement learning-driven ANN controller for microgrid energy management," *IEEE Trans. Smart Grid*, vol. 14, no. 2, pp. 1685–1697, 2023.
[40] F. Rossi and L. Greco, "Supervised LSTM network for solar irradiance forecasting in smart cities," *Energy AI*, vol. 12, 2023.